EasyChair Preprint

№ 8370

Numerical Analysis of Forced Convection in Rectangular Porous Channel

Ayush Gangil, Nishant Singh and Ram Vinoy Sharma

June 26, 2022

Proceedings of the 1st International Conference in Fluid Thermal and Energy Systems
June 9-11, 2022, NIT Calicut, Kerala, India
ICFTES2022–TS–042

Numerical Analysis of Forced Convection in Rectangular Porous Channel

Ayush Gangil[1*], Nishant Singh[1], Ram Vinoy Sharma[1]

[1]Department of Mechanical Engineering, NIT Jamshedpur, Jharkhand-831014, India
*Corresponding author email – ayushgangil@gmail.com

ABSTRACT

A numerical study on forced convection through horizontal rectangular channel filled with porous material has been carried out. Two-dimensional, laminar, and stable flow are considered in this research work. Darcy's law governs the flow. The top surface area is considered to be at constant temperature and convective heat transfer, whereas the bottom surface is considered to be an adiabatic surface. The gauge pressure at the outlet surface is assumed to be negligible. The governing equations and boundary conditions are rendered dimensionless. Peclet number (Pe), Aspect Ratio (AR) and Nusselt number (Nu) are the three dimensionless parameters in focus. Finite difference method has been incorporated to discretize the computational domain. The numerical solution was obtained using an explicit method. An original code in MATLAB was created for a variety of operational parameters, such as $1 \leq Pe \leq 10$ and AR 1 and 2, numerical tests have been carried out. A temperature profile (isotherm) was plotted. Additionally, the Nusselt number (Nu) and the effectiveness (ε) have been evaluated.

Temperature profiles, effectiveness, and the average Nusselt number are all influenced by parameters such as Peclet number and Aspect ratio. Effectiveness reduces when the Peclet number has increased, whereas the average Nusselt number begins to rise. Increases in effectiveness are accompanied by increases in aspect ratio and a reduction in the average Nusselt number.

Keywords: Porous media, Forced Convection, Darcy's law, Rectangular channel, explicit scheme

1. INTRODUCTION

Porous media has a wide range of study and we can study it with different shape of channels with different type of filling either continuous, partial or alternate blocks with applying different boundary conditions. A porous media is a material contains pores (voids). All solids and semi-solids contain interstitial spaces, when this space is sufficiently large and a flow can be established then it becomes porous. Porous material is mostly characterized by its porosity and permeability. Convection in porous media research has a wide range of applications, including geothermal power extraction, highly efficient composite heat exchangers, sensible storage beds, evaporative cooling, solar collectors, oil recovery by thermal method, and nuclear waste disposal technologies, among others (Karmakar et al., 2019; Sinha & Sharma, 2014)). The Darcy model was used to begin the exploration of porous media.(Darcy, 1856; Renken & Poulikakos, 1988) laid the foundation for performing recorded experiments and produce formulations pertaining to porous medium. The circulation of oil, water, and gas in porous materials is governed by Darcy's law. For laminar flow of an incompressible fluid in a solid non-deforming matrix of porous media, Darcy's law is applied. At any point within a reservoir, Darcy's law determines the flow rate based on the pressure gradient, viscosity , and effective permeability of the fluid. A theoretical study had investigated (Vafai & Tien, 1981) the forces of convection generated by a porous media boundary layer when there is a solid boundary and flow inertia. High Prandtl numbers, pressure gradients, and media with extremely permeable characteristics caused these consequences to be particularly strong at the leading edge of the boundary layer. In present study we consider a horizontal rectangular porous channel with top surface at constant temperature and keep bottom surface adiabatic. The fluid will flow from inlet to outlet with the help of pressure gradient and convective heat will transfer from top surface to the fluid and then we can get fluid with required temperature at the outlet by varying the parameters like Peclet number and Aspect ratio. Also we can obtain the output parameters like Average Nusselt number, Average outlet temperature and Effectiveness etc. by numerically experimentation.

2. LITERATURE REVIEW AND OBJECTIVE

(Huang & Vafai, 1994) investigated Brinkman-Forchheimer extended Darcy models to simulate force-driven convection in a channel with porous medium. Important fundamental and practical results have been presented and discussed. Results demonstrate how Reynolds number, Darcy number, Prandtl number, and inertial parameter affect the streamline, isotherm, and local Nusselt number distributions. Using the Brinkman-Forchheimer extended Darcy momentum equation, (Kuznetsov,

2001; Nield et al., 1996) investigated forced convection in a fluid-saturated porous-medium channel with isothermal limits. The results reveal (Lauriat and Ghafir, 2000) that when forced convection is fully developed in a fluid saturated porous media channel confined by parallel plates and a homogenous heat flux is given to the plates, the outcomes are as follows. The temperature profiles for each kind of boundary showed slight modification as a function of viscosity ratio fluctuations, Darcy number changes, and Forchheimer number changes. When Da or F were low, and particularly when M was small, temperature profiles increased considerably. As a result of the change in velocity profile, the Nusselt number is dramatically altered. Using the Darcy-Brinkman model, (Hooman & Merrikh, 2006) proposed an analytical expression for Forced Convection in a Rectangular Cross-sectional Duct Filled by a Porous Medium. Additionally, they examined Nusselt numbers versus shape factor (s) for different values of AR for small values of s and their effects on temperature and velocity distribution. The results show that the values of Nu for large aspect ratios clearly lie between those of clear flow and slug flow, as predicted. Regardless of AR value, Nu increases from a low to a high value as s increases from 10 to beyond s = 103. The forced convection in three-dimensional porous fin channels was studied numerically by (J. Yang et al., 2010) The flow and heat transmission in porous media are described using the (Davari & Maerefat, 2016; Fénot et al., 2008; Y.-T. Yang et al., 2016)Forchheimer-Brinkman extended Darcy model and the energy equation model. As the cold fluids, water and air are used and their effects on pin fin form and Reynolds number are studied. According to the findings of this study, porous pin fin channels may accomplish considerable pressure drop reduction and heat transmission increases with the correct selection of physical parameters. Furthermore, the total heat transfer performance of porous pin fin channels is far superior than that of solid pin fin channels. The impacts of pore density were also highlighted in this work.

After extensive and detailed study of available literature, it was observed that work on forced convection through porous channels governed by Darcy's law is rare in available literature. Moreover, the enthalpy balance model employed to calculate Nusselt's number is a novel approach addressed in the present study. In this study, the objective is to develop a mathematical model of forced convection through porous media, acquire a numerical solution, and analyze the impact of various parameters on the heat transfer process in a rectangular porous channel.

3. MATHEMATICAL MODEL

The temperature (Ti) and constant velocity (u) of the fluid pass through a porous rectangular channel with a length of L and a depth of H. The bottom wall is adiabatic, whereas the top wall is maintained at a constant temperature. Two-dimensional, stable, and laminar flow is assumed. Darcy's law governs the movement of fluids. Porous medium is isotropic & homogeneous. Thermal equilibrium is realized between fluid and solid inside the medium. Axial conduction is neglected. Lower surface is insulated and upper surface at constant temperature T_h and gauge pressure at outlet is zero.

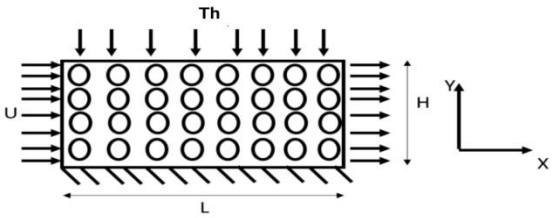

Figure 1: Physical model and coordinate system

The governing equations entail the conservation of mass, momentum, and energy as shown below;

$$\frac{\partial u}{\partial x}+\frac{\partial v}{\partial y}=0 \qquad (1)$$

$$\frac{\partial p}{\partial x}=-u\frac{K}{\mu} \qquad (2)$$

$$\frac{\partial p}{\partial y}=-v\frac{K}{\mu} \qquad (3)$$

$$\left[u\frac{\partial T}{\partial x}+v\frac{\partial T}{\partial y}\right]=\alpha\left[\frac{\partial^2 T}{\partial x^2}+\frac{\partial^2 T}{\partial y^2}\right] \qquad (4)$$

Initial boundary conditions:

At $x=0$ $\quad T=T_i$; At $x=L$ $\quad p=0$

At $y=0$ $\quad \frac{\partial T}{\partial y}=0$; At $y=H$ $\quad T=T_h$

Governing equation and boundary conditions are non-dimensionalised employing following non-dimensionalised variables:

$$U=\frac{u}{u_i}, \qquad V=\frac{v}{u_i}, \qquad X=\frac{x}{H},$$

$$Y=\frac{y}{H}, \qquad \theta=\frac{T-T_i}{T_h-T_I}, \qquad P=\frac{p}{\frac{\mu u_i H}{K}}$$

After non dimensionalisation Equation (1) to (4) becomes

$$\frac{\partial U}{\partial X}+\frac{\partial V}{\partial Y}=0 \qquad (5)$$

$$U=-\frac{\partial P}{\partial X} \qquad (6)$$

$$V=-\frac{\partial P}{\partial Y} \qquad (7)$$

$$Pe\left[U\frac{\partial \theta}{\partial X}+V\frac{\partial \theta}{\partial Y}\right]=\left[\frac{\partial^2\theta}{\partial X^2}+\frac{\partial^2\theta}{\partial Y^2}\right] \qquad (8)$$

Put equation (6) & (7) in equation (5) & (8) we get

$$\frac{\partial^2 P}{\partial X^2}+\frac{\partial^2 P}{\partial Y^2}=0 \quad (Laplace\ equation) \qquad (9)$$

$$\left[\frac{\partial^2\theta}{\partial X^2}+\frac{\partial^2\theta}{\partial Y^2}\right]+Pe\left[\frac{\partial P}{\partial X}.\frac{\partial \theta}{\partial X}+\frac{\partial P}{\partial Y}.\frac{\partial \theta}{\partial Y}\right]=0 \qquad (10)$$

Boundary conditions after non dimensionalisation

At $X=0$ $\quad \theta=0$; At $X=AR$ $\quad P=0$

At $Y=0$ $\quad \frac{\partial \theta}{\partial Y}=0$; At $Y=1$ $\quad \theta=1$

4. NUMERICAL SCHEME

An explicit scheme has been used to solve equation (10) with boundary conditions. Finite Difference Method has been exercised to discretize computational domain as depicted in Fig.2

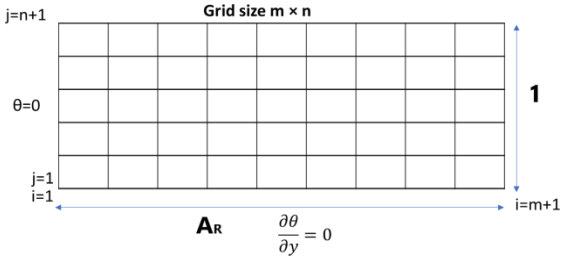

Figure 2: Meshing in a computational domain

If m and n are the number of horizontal (x) and vertical (y) divisions, then the interspacing distance will be:

$$\Delta X=\frac{AR}{m}\ ,\quad \Delta Y=\frac{1}{n} \qquad (11)$$

The Laplace equation (9) can be solved analytically with the help of boundary conditions from where we get

$$P=AR-X \qquad (12)$$

The equation (10) in finite difference form after neglecting axial conduction becomes

$$\frac{\theta_{i,j+1}-2\theta_{i,j}+\theta_{i,j-1}}{\Delta Y^2}+Pe\left[\left(\frac{P_{i+1,j}-P_{i-1,j}}{2\Delta X}\right).\left(\frac{\theta_{i+1,j}-\theta_{i,j}}{\Delta X}\right)+\left(\frac{P_{i,j+1}-P_{i,j-1}}{2\Delta Y}\right).\left(\frac{\theta_{i,j+1}-\theta_{i,j-1}}{2\Delta Y}\right)\right]=0 \qquad (13)$$

Boundary conditions after discretization are

At $i=0$ $\quad \theta_{0,j}=0;$ $\quad$ At $i=m$ $\quad P_{m,j}=0$

At $j=0$ $\quad \theta_{i,0}=(4\theta_{i,1}-\theta_{i,2})/3;$ At $j=n$ $\quad \theta_{i,n}=1$

In present study we employed the explicit scheme so there should be stability criteria to make equation stable and valid after discretization.

$$\theta_{i,j+1}=\theta_{i,j}+\frac{\Delta X}{Pe.\Delta Y^2}\left(\theta_{i,j+1}-\theta_{i,j}+\theta_{i,j-1}\right)$$

$$\theta_{i,j+1}=\frac{r}{Pe}\left(\theta_{i,j+1}+\theta_{i,j-1}\right)+\left(1-\frac{2r}{Pe}\right)\theta_{i,j}$$

Here $r=\frac{\Delta X}{\Delta Y^2}$ so for stability $r\le\frac{Pe}{2}$

$$r=\frac{\Delta X}{\Delta Y^2}=\frac{AR.n^2}{m}\le\frac{Pe}{2} \qquad (14)$$

4.1 Effectiveness ($\mathcal{E}$)

$$\text{Effectiveness }(\mathcal{E})=\frac{\text{Actual Heat Transfer}}{\text{Max. Heat Transfer}}=\frac{\dot{m}c_p(T_o-T_i)}{\dot{m}c_p(T_h-T_i)}$$

Avg. Outlet Temperature (θ_{avg}) = Effectiveness = θ_0

By Simpson's one third rule of numerical integration, we can solve

$$\text{Effectiveness }(\mathcal{E})=\theta_{avg}=\frac{1}{1}\int_0^1\theta_j.dY$$

$$\int_0^1\theta_j\,.dY=[\theta_{m,1}+\theta_{m,n+1}+4\sum_{j=2,4,6\ldots}^{n-1}\theta_{m,j}+2\sum_{j=3,5,7\ldots}^{n-1}\theta_{m,j}] \qquad (15)$$

4.2 Nusselt number calculation

Heat loss by top surface = Heat gain by fluid

$$Q=h.A_s.LMTD=\dot{m}\,c_p\,(T_o-T_i) \qquad (16)$$

$$\text{Avg. Nusselt No. }(Nu_{avg})=\frac{h.H}{K}=\frac{\dot{m}c_p(T_o-T_i)}{(As.LMTD).\frac{H}{K}}$$

Here $A_s=L*1,$ $\quad \dot{m}=\rho*H*U$ $\quad$ &

$$LMTD=\frac{(T_h-T_i)-(T_h-T_o)}{ln\frac{(T_h-T_i)}{(T_h-T_o)}}=\frac{T_o-T_i}{ln\left(\frac{1}{1-\theta_{avg}}\right)}$$

Avg. Nusselt No. (Nu_{avg})

$$Nu_{avg}=\frac{Pe}{AR}.ln\left(\frac{1}{1-\theta_{avg}}\right) \qquad (17)$$

5. RESULTS

A grid optimization test was performed to determine the best grid size for Peclet number 10. Grid size of

320x40 and 640 x40 has been found to be optimum for Aspect ratio 1 and 2 respectively. As shown in Table 1 and 2 there is negligible change in Average Nusselt number and Effectiveness for grid size with n=40. All computations were done with a grid size of n=40.

Table 1: Grid Optimization Test For *Pe*=10 , *AR*=1

S. No.	Grid Size (m×n)	Nu_{avg}	$\mathcal{E} = \theta_{avg}$
1	20×10	4.435	0.360
2	80×20	4.420	0.357
3	320×40	4.415	0.357
4	1280×80	4.414	0.357

Table 2: Grid Optimization Test For *Pe*=10, *AR*=2

S. No.	Grid Size (m×n)	Nu_{avg}	$\mathcal{E} = \theta_{avg}$
1	40×10	3.521	0.505
2	160×20	3.510	0.504
3	640×40	3.507	0.504
4	2560×80	3.507	0.504

A variety of different operational parameters, including Peclet number (Pe: 1–10) and aspect ratios (AR: 1.0 & 2.0), have been numerically tested. Such variables' influences on temperature fields, average Nusselt number, and effectiveness have all been discussed. The depth of temperature penetration reduces as the Peclet number increases (Fig.4 to Fig.7). This is due to an increase in convection strength. As aspect ratio increases (Fig.8), Average Nusselt number decreases hence temperature penetration decreases.

By equation (12) the pressure field obtained for *P=AR-X*.

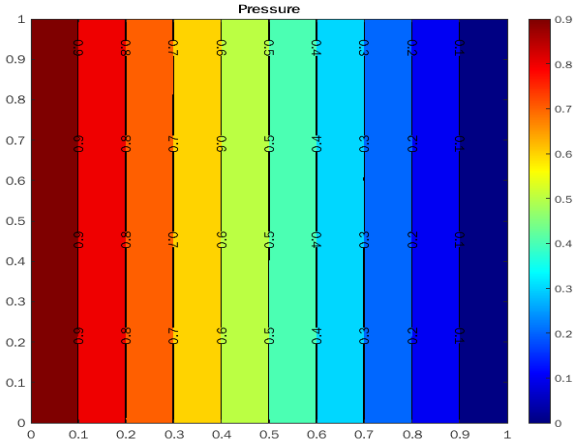

Figure 3: Pressure field for Aspect Ratio =1

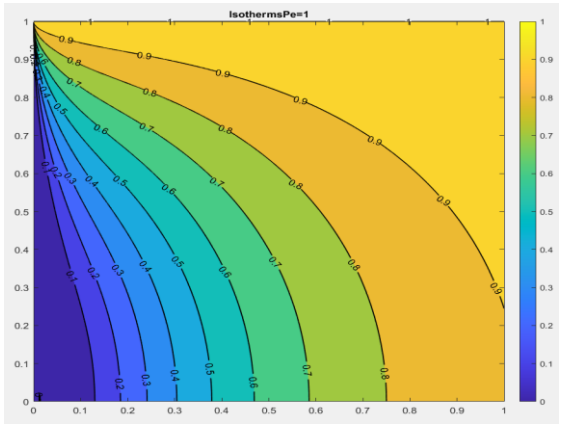

Figure 4: Temperature profile for *Pe*=1, *AR*=1

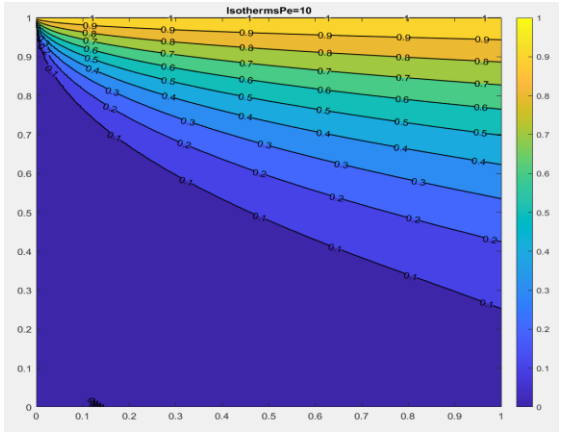

Figure 5: Temperature profile for *Pe*=10, *AR*=1

The Peclet number is the ratio of advection to diffusion. As a result, as the Peclet number increases, advection increases, implying that convective heat transfer dominates conductive heat transfer, as illustrated in figs. 4 and 5. As it is indicated from fig.4 and fig.5, initially the gaps between isotherms are very narrow, i.e. there is more heat transfer than the points when it gets spacious.

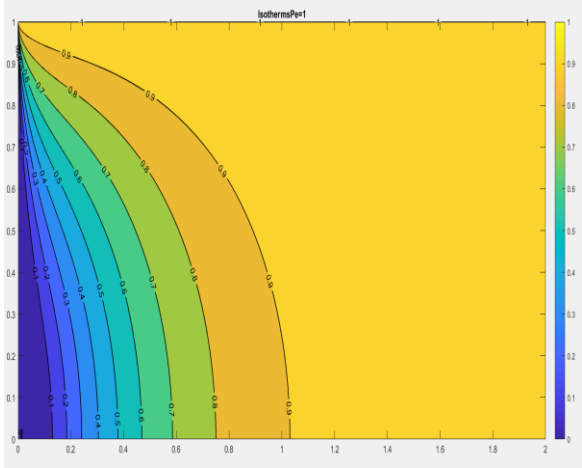

Figure 6: Temperature profile for *Pe*=1, *AR*=2

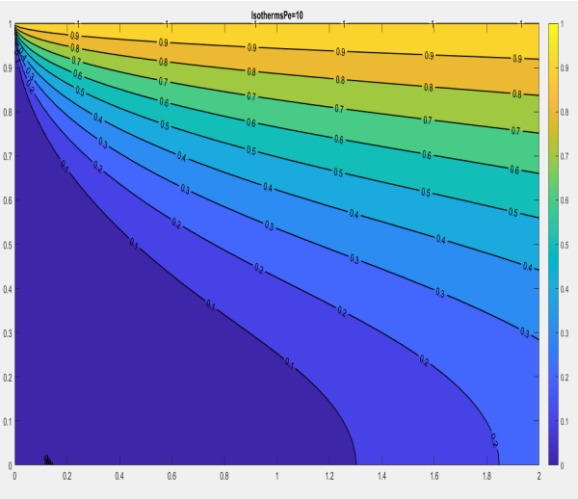

Figure 7: Temperature profile for *Pe*=10, *AR*=2

Effects of different parameters on Average Nusselt number and effectiveness have been recorded by doing numerical experiments and shown in Figure 8 and Figure 9.

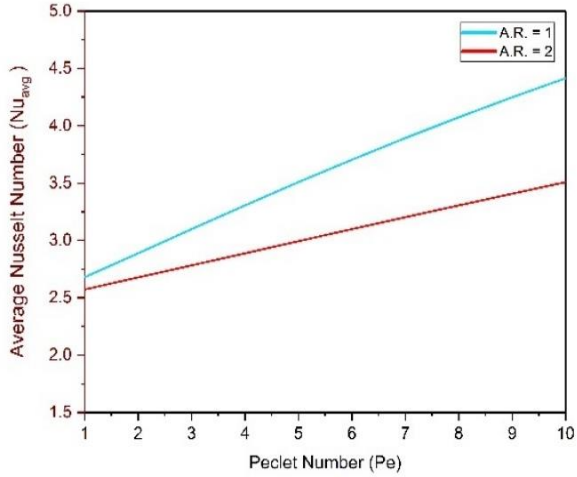

Figure 8: Avg. Nusselt No.(Nu_{avg}) vs Peclet No.(*Pe*) at Different *AR*

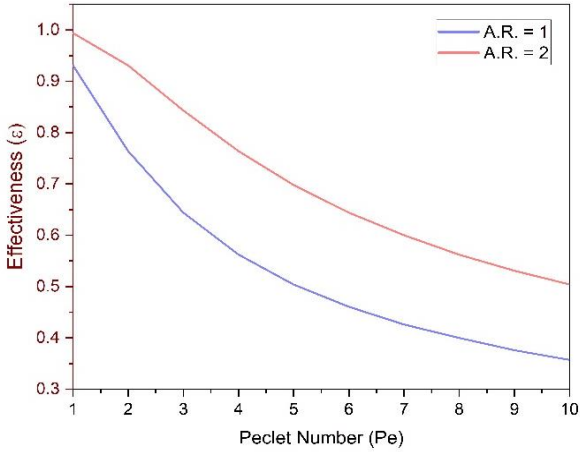

Figure 9: Effectiveness ($\mathcal{E}$) vs Peclet No. (*Pe*) at Different *AR*

6. CONCLUSIONS

After extensive study and numerical experimentation, the following conclusions have been listed below:

1. As Peclet No. increases, Avg Nusselt No. Increases and Effectiveness decreases.
2. For same Peclet No., Avg Nusselt No. is higher on less Aspect Ratio and lower on high Aspect Ratio.
3. For same Peclet No. Effectiveness is higher on high Aspect Ratio and lower on low Aspect Ratio.
4. As Peclet No. increases, Avg Nusselt No. increases rapidly on low Aspect Ratio in comparison to high Aspect Ratio.
5. As Aspect Ratio increases, Avg Nusselt No. decreases and Effectiveness increases.
6. For same Aspect Ratio, Avg Nusselt No. is higher at high Peclet no. and lower at low Peclet no.
7. For same Aspect Ratio, Effectiveness is higher at low Peclet no. and lower at high Peclet no.
8. As Aspect Ratio increases, Avg Nusselt No. decreases rapidly on high Peclet no. in comparison to low Peclet no.
9. As Aspect Ratio increases, Effectiveness increases rapidly on low Peclet no. in comparison to high Peclet number.

The boundary conditions employed in this analysis do not have any real practical examples, but this case is very similar to the solar collector. Although the top surfaces of solar collectors have a constant flux, it was theoretically assumed that they are isothermal to avoid complications and simplify the numerical study of forced convection in porous channels. The top surface is assumed to be isothermal if there is any phase change or the heat transfer coefficient value is very high. This is an ideal case where we use the Dirichlet boundary condition for better study of numerical analysis.

NOMENCLATURE

A	Area	[m^2]
AR	Aspect ratio	--
C_p	Specific heat capacity	[J/kgK]
$\mathcal{E}$	Effectiveness	--
h	Convective heat transfer coefficient	[W/m^2K]
H	Height	[m]
k	Thermal conductivity	[W/mK]
K	Permeability	[m^2]
L	Length	[m]
m	Number of partitions in x-axis	--
$\dot{m}$	Mass flow rate	[kg/s]
n	Number of partitions in y-axis	--

Nu	Nusselt number	--
p	Gauge pressure	[Pa]
P	Dimensionless pressure	--
Pe	Peclet number	--
r	Stability criteria	--
T	Temperature	[K]
u	x-axis velocity	[m/s]
U	Dimensionless x-axis velocity	--
v	y-axis velocity	[m/s]
V	Dimensionless y-axis velocity	--
x	Horizontal direction	[m]
X	Dimensionless horizontal direction	--
y	Vertical direction	[m]
Y	Dimensionless vertical direction	--

Greek letters

μ	Dynamic viscosity	[Ns/m^2]
ρ	Density of fluid	[kg/m^3]
θ	Dimensionless temperature	--
α	Thermal diffusivity	[m^2/s]

Suffixes

avg	Average
f	Fluid
h	Hot
i	Inlet
o	Outlet

REFERENCES

Darcy, H. (1856). *Les fontaines publiques de la ville de Dijon: exposition et application...* Victor Dalmont.

Davari, A., & Maerefat, M. (2016). Numerical analysis of fluid flow and heat transfer in entrance and fully developed regions of a channel with porous baffles. *Journal of Heat Transfer*, *138*(6).

Fénot, M., Dorignac, E., & Vullierme, J.-J. (2008). An experimental study on hot round jets impinging a concave surface. *International Journal of Heat and Fluid Flow*, *29*(4), 945–956.

Hooman, K., & Merrikh, A. A. (2006). *Analytical solution of forced convection in a duct of rectangular cross section saturated by a porous medium.*

Huang, P. C., & Vafai, K. (1994). Analysis of forced convection enhancement in a channelusing porous blocks. *Journal of Thermophysics and Heat Transfer*, *8*(3), 563–573.

Karmakar, T., Reza, M., & Sekhar, G. P. R. (2019). Forced convection in a fluid saturated anisotropic porous channel with isoflux boundaries. *Physics of Fluids*, *31*(11), 117109.

Kuznetsov, A. v. (2001). Influence of thermal dispersion on forced convection in a composite parallel-plate channel. *Zeitschrift Für Angewandte Mathematik Und Physik ZAMP*, *52*(1), 135–150.

Nield, D. A., Junqueira, S. L. M., & Lage, J. L. (1996). Forced convection in a fluid-saturated porous-medium channel with isothermal or isoflux boundaries. *Journal of Fluid Mechanics*, *322*, 201–214.

Renken, K. J., & Poulikakos, D. (1988). Experiment and analysis of forced convective heat transport in a packed bed of spheres. *International Journal of Heat and Mass Transfer*, *31*(7), 1399–1408.

Sinha, M. K., & Sharma, R. v. (2014). Influence of Property Variation on Natural Convection in a Gas Saturated Spherical Porous Annulus. *Transport in Porous Media*, *104*(3), 521–535.

Vafai, K., & Tien, C. L. (1981). Boundary and inertia effects on flow and heat transfer in porous media. *International Journal of Heat and Mass Transfer*, *24*(2), 195–203.

Yang, J., Zeng, M., Wang, Q., & Nakayama, A. (2010). *Forced convection heat transfer enhancement by porous pin fins in rectangular channels*.

Yang, Y.-T., Tsai, K.-T., Tang, H.-W., & Chung, S.-E. (2016). Numerical simulations and optimization of porous pin fins in a rectangular channel. *Numerical Heat Transfer, Part A: Applications*, *70*(7), 791–808.